Automated and ImageJ thresholding algorithm-based analysis of macular vessel density in diabetic patients

Devesh Kumawat, Rohan Chawla, Pooja Shah, Anu Sharma, Anusha Sachan, Veena Pandey[1]

Purpose: To assess the macular vessel density (VD) on optical coherence tomography angiography (OCT-A) using proprietary software (automated) and image processing software (manual) in diabetic patients. **Methods:** In a retrospective study, OCT-A images (Triton, TOPCON Inc.) of type 2 diabetics presenting to a tertiary eye care center in North India between January 2018 and December 2019 with or without nonproliferative diabetic retinopathy (NPDR) and with no macular edema were analyzed. Macular images of size 3 × 3 mm were binarized with global thresholding algorithms (ImageJ software). Outcome measures were superficial capillary plexus VD (SCP-VD, automated and manual), deep capillary plexus VD (DCP-VD, manual), and correlation between automated and manual SCP-VD. **Results:** OCT-A images of 89 eyes (55 patients) were analyzed: no diabetic retinopathy (NoDR): 29 eyes, mild NPDR: 29 eyes, and moderate NPDR: 31 eyes. Automated SCP-VD did not differ between NoDR and mild NPDR ($P = 0.69$), but differed between NoDR and moderate NPDR ($P = 0.014$) and between mild and moderate NPDR ($P = 0.033$). Manual SCP-VD (Huang and Otsu methods) did not differ between the groups. Manual DCP-VD differed between NoDR and mild NPDR and between NoDR and moderate NPDR, but not between mild and moderate NPDR with both Huang ($P = 0.024$, 0.003, and 0.51, respectively) and Otsu ($P = 0.021$, 0.006, and 0.43, respectively) methods. Automated SCP-VD correlated moderately with manual SCP-VD using Huang method ($r = 0.51$, $P < 0.001$) with a mean difference of −0.01% (agreement limits from −6.60% to +6.57%). **Conclusion:** DCP-VD differs consistently between NoDR and NPDR with image processing, while SCP-VD shows variable results. Different thresholding algorithms provide different results, and there is a need to establish consensus on the most suited algorithm.

Key words: Capillary Plexus Vessel Density, diabetic retinopathy, ImageJ processing software, optical coherence tomography angiography, thresholding algorithm

Optical coherence tomography angiography (OCT-A) is a noninvasive tool to study the retinal and choroidal microvasculature both qualitatively and quantitatively at different depths without the need for dye injection.[1] OCT-A has been used extensively in various ocular disorders such as age-related macular degeneration, diabetic eye disease, macular telangiectasia, and central serous chorioretinopathy to characterize the abnormalities in the retinal and choroidal circulation. Apart from this, there is growing evidence of correlation between quantitative assessment of retinal vasculature on OCT-A and disease severity in systemic diseases such as systemic lupus erythematosus and Alzheimer's disease.[2,3]

OCT-A has become an important tool for the assessment of retinopathy in diabetic patients. Use of OCT-A for the evaluation of morphological changes in diabetic retinopathy (DR), such as preretinal neovascularization and the quantification of foveal avascular zone, capillary nonperfusion area, and macular capillary vessel density (VD), has been described in various studies.[1,4,5] Many instruments have become available for performing OCT-A with pros and cons of each other.[6] Each one has its proprietary software to calculate the macular capillary VD.[1,7–10] The potential utility of VD assessment of healthy and diseased eyes using such an instrument has been suggested previously.[1] However, the results may vary to a certain extent between the devices, and each one of these devices may have their particular strengths and weakness.[6] Also, quantitative automated depth-resolved analysis of VD may not be available for all devices. In such cases, numerous authors have used different thresholding algorithms on to the images captured by the device and have analyzed the VD manually.[11–19]

ImageJ is a Java system used for image processing.[20] ImageJ-based thresholding algorithms have been used recently to quantitatively analyze the retinal and choroidal vasculature.[11,14,17–19] The thresholding algorithm can be either

Dr. Rajendra Prasad Centre for Ophthalmic Sciences, All India Institute of Medical Sciences, New Delhi, [1]Department of Biostatistics, Dr. Rajendra Prasad Centre for Ophthalmic Sciences, All India Institute of Medical Sciences, New Delhi, India

Correspondence to: Dr. Rohan Chawla, Dr. Rajendra Prasad Centre for Ophthalmic Sciences, All India Institute of Medical Sciences, New Delhi - 110 029, India. E-mail: dr.rohanrpc@gmail.com

global (same threshold value applied across the entire image) or local/adaptive (different threshold values to various areas of image). Global Otsu method has been uniformly used in a few studies assessing the retinal and choroidal vasculature in diabetic patients.[13,14,17] Another global method, Huang, has been found to be superior to Otsu for thresholding microscopic images depicting drug distribution in living cells.[21]

It is not known if a particular algorithm is superior to the other when OCT-A images of retinal vasculature are considered. Since there is no gold-standard technique to which these algorithms can be compared, the diagnostic ability of each one of these in itself is limited. Also, no studies have compared the proprietary automated analysis and thresholding algorithm-based analysis of the macular VD.

Previous studies have consistently shown that the VD differs between eyes with no DR (NoDR) and proliferative DR (decreasing in proliferative cases),[22–24] but the results are conflicting when a comparison is made between NoDR and mild/moderate nonproliferative DR (NPDR).[22–24] It also remains unclear if the VD changes significantly with increasing severity from mild to moderate/severe disease.[22–24]

We performed a retrospective study to identify if any difference exists in macular VD across the spectrum of DR and to determine the correlation between automated and thresholding algorithm-based methods of VD analysis.

Methods

We performed a retrospective review of records of type 2 diabetic patients who presented to the retina clinic of our tertiary eye care center in North India over a period from January 2018 to December 2019. The study was carried out in accordance with the tenets of the Declaration of Helsinki. Ethical clearance was obtained from the institutional research committee.

Study population

At the retina clinic, patients with type 2 diabetes are screened for DR changes and presence of diabetic macular edema (DME) using biomicroscopic examination. Baseline fundus imaging and optical coherence tomography (DRI OCT Triton, TOPCON Inc.) are performed, wherever possible. We searched the retina clinic records for emmetropic diabetic patients with or without mild–moderate NPDR with clear ocular media and distance visual acuity ≥20/20 and their ocular imaging was reviewed. The diagnosis of the severity of DR was made as per the International Clinical DR and DME severity scale. The exclusion criteria included presence/history of DME, previous treatment for DR/DME, history of hypertension, any other retinal vascular pathology, glaucoma, age-related macular degeneration, cataract surgery within the last 6 months, and history of retinal surgery.

The patients were divided based on the retinal examination findings into three groups: diabetes with NoDR, mild NPDR, and moderate NPDR. The demography, age/sex of the patients, and duration of diabetes were noted.

Imaging

The OCT-A images on DRI OCT device (Triton, TOPCON Inc.) were reviewed. Artifact (projection/shadow/blink)-free 3 × 3 mm macular cube images with centration on the foveal avascular zone and good signal strength (>6/10) were selected; else, the eyes were excluded. IMAGEnet software-based enface images were segmented automatically to define the superficial retinal capillary plexus (SCP) and deep retinal capillary plexus (DCP).[25]

Automated VD

The built-in software provided the VD for SCP separately for the foveal region (central 1 mm circle) and four quadrants (superior, nasal, inferior, and temporal) of the parafoveal region (centered on fovea with inner and outer ring diameters of 1 and 3 mm, respectively) in the form of Early Treatment of Diabetic Retinopathy Study (ETDRS) grid [Fig. 1a]. The grid was checked for centration on to the fovea. The software calculates VD in the form of the percentage of area occupied by the vessels. The software does not provide a single VD value for the whole grid. As the inner circle/foveal region comprises the foveal avascular zone, which is devoid of vessels and may vary with the severity of DR,[22,26] the average density was estimated including the foveal area as well as the parafoveal area. A mathematical average of the central/foveal and parafoveal VD values (accounting for the different areas of these regions) was calculated by the examiner (AS) to determine a single VD value for the grid and termed as "average automated VD."

Manual quantification using image processing

The enface images were exported to ImageJ 1.48v software (National Institute of Health, Bethesda, MD, USA).[20] The analysis was performed separately for the SCP [Fig. 1b-f] and DCP images by a single examiner (DK). The images were binarized using manual global thresholding

Table 1: Clinical characteristics and macular vessel density measured with TOPCON DRI OCT instrument (3×3 mm scan)

Characteristic	Value
Patients, *n*	55
Eyes, *n*	89
Sex	
Male, *n* (%)	34 (61.8)
Female, *n* (%)	21 (38.2)
Age (years), mean±SD	53.3±10.1
Diabetes duration (years), mean±SD (median, range)	9.3±7.2 (8, 1-37)
Automated vessel density (percentage), mean±SD	
Whole area (3×3 mm)	43.8±2.3
ImageJ thresholding algorithm-based vessel density (percentage), mean±SD	
Superficial plexus, Huang algorithm	43.4±3.1
Superficial plexus, Otsu algorithm	27.6±4.4
Superficial plexus: larger vessels, Maximum entropy algorithm	8.5±1.8
Superficial plexus: smaller vessels, Huang minus Maximum entropy algorithm	35.0±3.1
Superficial plexus: smaller vessels, Otsu minus Maximum entropy algorithm	19.1±4.7
Deep plexus, Huang algorithm	41.2±1.6
Deep plexus, Otsu algorithm	30.6±3.0

OCT=optical coherence tomography, SD=standard deviation
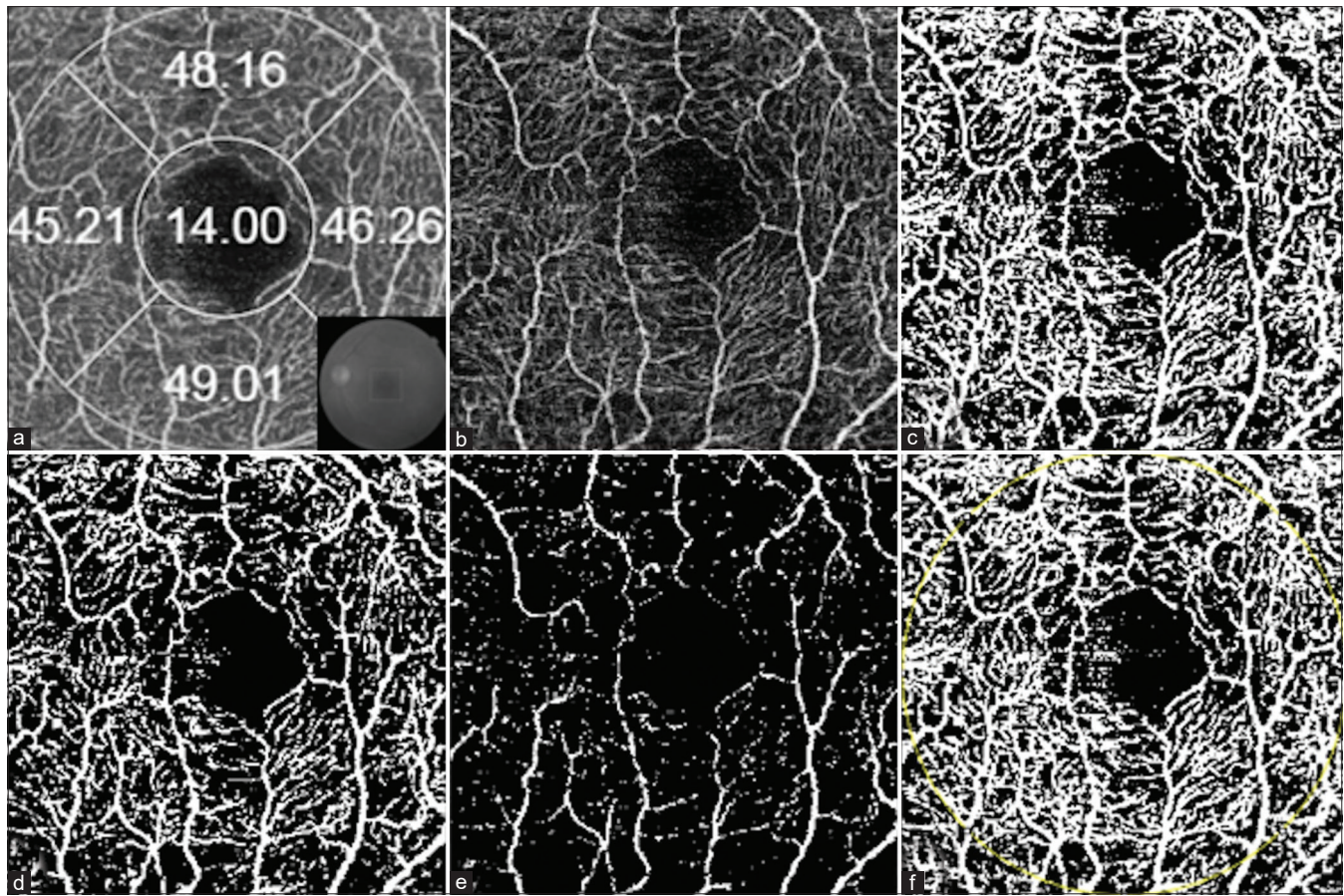
Figure 1: Representative OCT-A images of left eye superficial retinal capillary plexus. (a) Automated vessel density values in inner foveal and outer parafoveal regions of 3 × 3 mm ETDRS grid. (b) Superficial capillary plexus image. Outputs of different thresholding algorithms on Image J software are shown in (c) Huang, (d) Otsu, and (e) Maximum entropy. (f) Fit circle selection is taken centered on fovea of the size 3 mm for the Huang output image. Finally, histogram analysis of the white and black pixels is done for each algorithm output image (pixels in selection area- 66,076, white pixel on Huang image- 27,946, white pixel on Otsu image- 19,039, white pixel on Maximum entropy image- 5894). OCT-A = optical coherence tomography angiography

algorithms (Otsu and Huang), as the OCT-A images tend to be evenly illuminated. A circular area of 3 mm diameter was selected, centered on the foveal avascular zone. The histogram of image intensity was analyzed for the pixel count of the white (vessels) and dark areas (devoid of the vessel) in the selected area. The explant/selected image area was noted in the form of total pixel count. The VD was calculated as a percentage (the pixel count of white regions divided by the pixel count of explant area multiplied by 100). We also studied the larger vessels in superficial plexus by applying the Maximum entropy algorithm. The retinal perfusion occurs at the level of capillaries and not the larger vessels. Therefore, it becomes important to determine the VD of larger vessels and subtract it from the total VD. The VD of larger vessels for a given OCT-A image was subtracted from the total VD to estimate the VD of smaller vessels where the actual retinal perfusion occurs.

Statistical analysis

The statistical analysis was performed using Statistical Package for the Social Sciences (SPSS) 21.0 software. The parametric data (age and VD) was compared between the groups with Student's t test or analysis of variance (ANOVA). The nonparametric data (duration of diabetes) was compared between the groups with Mann–Whitney test or Kruskal–Wallis
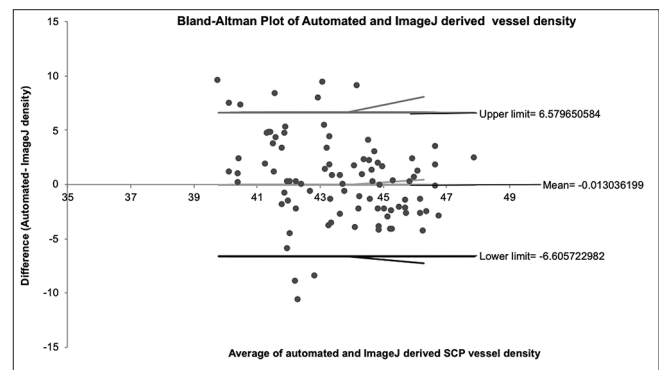
Figure 2: Bland–Altman plot of the difference in SCP vessel density calculated automatically by the instrument in the 3 × 3 mm ring of ETDRS grid and that derived from ImageJ-based Huang thresholding algorithm (mean difference – 0.01, 95% CI – 0.40 to 1.20, 95% limits of agreement – 6.60, +6.57). CI = confidence interval, SCP = superficial capillary plexus

test. Bonferroni correction was used to adjust for multiple comparisons. The categorical data distribution (sex) was studied with Pearson's Chi-square test. Both eyes were included for some subjects, while in others only one eye was included.

Table 2: Comparison of macular vessel density measured with TOPCON DRI OCT instrument (3×3 mm scan) in different grades of diabetic retinopathy

	NoDR	Mild NPDR	Moderate NPDR	P# (multiple comparisons between NoDR, mild NPDR, and moderate NPDR)	P# (comparison between NoDR and mild NPDR)	P# (comparison between NoDR and moderate NPDR)	P# (comparison between mild and moderate NPDR)
Patients, *n*	19	16	20	-	-	-	-
Eyes, *n*	29	29	31	-	-	-	-
Sex				-	-	-	-
Male, *n* (%)	10 (52.6)	9 (56.3)	15 (75)	0.30			
Female, *n* (%)	9 (47.4)	7 (43.7)	5 (25)				
Age (years), mean±SD	54.5±10.7	54.2±7.5	51.5±11.5	0.59	-	-	-
Diabetes duration (years), mean±SD (median, range)	4.9±3.7 (3, 1-12)	12.0±9.3 (10, 1-37)	11.4±6.0 (10.5, 1-24)	<0.001	-	-	-
Automated vessel density (percentage), mean±SD							
Whole area (3×3 mm)	44.5±1.8	44.3±2.0	42.8±2.6	0.025	0.69	0.014	0.033
ImageJ thresholding algorithm-based vessel density (percentage), mean±SD							
Superficial plexus, Huang	44.4±3.0	43.1±3.0	42.8±3.2	0.16	0.21	0.06	0.51
Superficial plexus, Otsu	27.3±5.3	28.0±4.7	27.4±3.2	0.93	0.74	0.97	0.74
Superficial plexus: larger vessels, Maximum entropy	8.3±1.9	8.7±2.1	8.4±1.3	0.88	0.62	0.81	0.77
Superficial plexus: smaller vessels, Huang minus Maximum entropy	36.2±3.4	34.5±2.7	34.4±3.1	0.10	0.08	0.051	0.77
Superficial plexus: smaller vessels, Otsu minus Maximum entropy	19.0±5.8	19.4±4.7	18.9±3.4	0.97	0.87	0.94	0.81
Deep plexus, Huang	42.4±2.4	40.7±2.0	40.5±3.0	0.01	0.024	0.003	0.51
Deep plexus, Otsu	32.0±2.7	29.8±2.5	30.1±3.2	0.01	0.021	0.006	0.43

DR=diabetic retinopathy, NoDR=no diabetic retinopathy, NPDR=nonproliferative diabetic retinopathy, OCT=optical coherence tomography, SD=standard deviation

#Generalized estimating equation was applied to take care of the clustering effect

This was done to take care of poor-quality images in one eye of certain subjects and to have a reasonable sample size. Taking care of this clustering effect, generalized estimating equation was used to compare the parameters between the groups. The correlation between the automated and manual VD was studied with Pearson's correlation test. The difference between the automated and manual VD was analyzed using Bland–Altman plot. A P value of <0.05 was deemed statistically significant.

Results

OCT-A images of 89 eyes of 55 patients were included in this study. The clinical characteristics of the entire study sample are given in Table 1. The distribution in different groups was as follows: 29 eyes each in NoDR and mild NPDR groups and 31 eyes in moderate NPDR group [Table 2]. The mean age was 53.3 ± 10.1 years (range 30–74 years). The age distribution was not statistically different between the groups (P = 0.59) [see Table 2]. Thirty-four patients were male, and the rest 21 patients were female with no significant difference in distribution between the groups (P = 0.30). The mean duration of diabetes was 9.3 ± 7.2 (median 8, range 1–37 years). The mean duration was significantly greater in NPDR groups compared to NoDR group, but the difference between the mild and moderate NPDR groups was not significant (P = 0.20) [see Table 2].

Superficial retinal capillary plexus vessel density

The mean average automated SCP-VD was 43.8 ± 2.3 [Table 1]. There was statistically significant difference between the groups on multiple comparison test (P = 0.025) [see Table 2], with a decrease in density observed with increasing severity of disease from mild to moderate NPDR. However, no significant difference was observed in automated SCP-VD between NoDR and mild NPDR groups (P = 0.69).

The mean manual SCP-VDs calculated as per the Huang and Otsu methods were 43.4 ± 3.1 and 27.6 ± 4.4, respectively [Table 1]. On multiple comparison, significant difference was not noted between the DR groups as per the Huang method (P = 0.16) as well as the Otsu method (P = 0.93) [see Table 2].

The mean VD of larger vessels in SCP calculated as per the Maximum entropy method was 10.0 ± 1.7, and the difference was not significant between the groups on multiple comparison (P = 0.88) [see Table 2]. Although not significant, the VD of larger vessels was greater in mild DR group (8.7 ± 2.1) compared to NoDR (8.3 ± 1.9) and moderate DR (8.4 ± 1.3) groups. The VD of smaller vessels (after subtraction of VD of larger vessels form total VD) was also not different between the groups with the Huang method (P = 0.10) as well as the Otsu method (P = 0.97) [see Table 2]. However, the difference in VD of smaller vessels between NoDR and moderate NPDR was just short of significance (P = 0.051) [see Table 2].

Deep retinal capillary plexus vessel density

The mean manual DCP-VDs calculated as per the Huang and Otsu methods were 41.2 ± 1.6 and 30.6 ± 3.0, respectively. On multiple comparison, a significant difference was noted between the groups as per both the methods (P = 0.01 and 0.01, respectively) [see Table 2]. However, on two-sample comparison, the difference was only significant between NoDR and mild NPDR groups and not between mild and moderate NPDR groups [Table 2].

Correlation and comparison of automated and manual density in SCP

Moderately strong correlation was noted between the automated and manual VDs, both with the Huang method (r = 0.51, 95% confidence interval [CI] 0.34–0.65; P < 0.001) and the Otsu method (r = 0.50, 95% CI 0.33–0.64; P < 0.001). On direct comparison, there was no statistically significant difference between automated VD and manual VD using the Huang method (P = 0.15) in SCP (P = 0.15), but the Otsu-based VD values were significantly lower than automated VD (P < 0.001). The level of agreement was studied between the automated VD and the Huang-based manual VD. On Bland–Altman analysis, the mean difference between these was − 0.01 (95% CI − 0.40 to 1.20) and the 95% limits of agreement were − 6.60 and + 6.57 [Fig. 2].

Discussion

The retinal vasculature has been extensively studied in healthy and diseased eyes. The means of quantification include automated analysis inherent of the measuring instrument and manual image analysis methods. ImageJ is a public domain software developed by National Institutes of Health (NIH) and used for image processing.[20] ImageJ uses different thresholding methods to binarize the images. Otsu method is a commonly used clustering method.[21,27] It separates the image pixels into two groups after analyzing the global intensity, such that the intergroup variance remains very high and the intragroup variance remains very low.[27] Otsu method has been used previously in diabetic patients to compare the VD between various grades of DR, and its reliability and repeatability have been established.[14,17]

It remains unclear if the VD values obtained with the Otsu method truly represent the actual VD. Otsu method is effective in conditions where the foreground and the background brightness remain similar.[21] However, this may not follow in case of retinal vasculature where the brightness intensity will vary depending upon the caliber of the vessels and the flow in these vessels. Huang method is an object attribute method which segments based on certain similarities of the object feature.[21,28] It minimizes the measures of fuzziness of an image.[28] Giedt et al.[21] found Huang method to be superior to Otsu method when there are multiple levels of brightness in the image. However, their analysis was based on identification of fluorescently labeled drugs in intravital imaging and not using OCT-A images. In our study, a moderately strong correlation was noted between the automated VD and manual VD as per both the Huang and Otsu methods. But unlike the Otsu method, the Huang method provided VD results statistically similar to the automated results.

The retinal vasculature includes the large superficial vessels (first- and second-order vein and arteries) and smaller superficial and deep capillary plexus. The retinal perfusion occurs at the level of capillaries and not the larger vessels. Therefore, it becomes important to determine the VD of larger vessels and subtract it from the total VD. Also, the large venule caliber varies with the severity of NPDR,[29,30] and thus, the estimated VD may be falsely interpreted if the larger vessels are not taken into account. The AngioVue instrument has updated software which calculates the VD after subtracting the larger vessel effect.[31] VD of larger retinal vessels has not been estimated previously using the ImageJ processing software.

We used Maximum entropy algorithm for this purpose. Maximum entropy algorithm is similar to the Otsu method, but instead of maximizing the intergroup variance, it maximizes the intergroup entropy.[32,33] Another way of analysis is to use the skeleton images after performing segmentation instead of subtracting the larger vessels.[13] Some authors believe that since the nutritional flux occurs along the vessel wall, the vessel length, but not the caliber, may be more important.[13] However, in our opinion, this may underestimate the VD and even while using this method, care should be taken while comparing values between different machines/studies.

In our study, we found a significant difference in automated SCP-VD between NoDR and moderate NPDR groups and between mild NPDR and moderate NPDR groups, but not between NoDR and mild NPDR groups. However, while using the Huang and Otsu algorithms, there was no statistically significant difference in manual SCP-VD between the groups. Thus, the results of SCP-VD using various approaches appear inconsistent. When we subtracted the VD of large vessels and compared the VD of small vessels in SCP, we found that the difference in VD between NoDR and moderate NPDR approached toward significance (P = 0.51). This may have reached significance if our sample size was larger. It is possible that the difference in VD of small vessels in SCP may be appreciable only after development of moderate NPDR changes. Another interesting observation was that VD of larger vessels in SCP was greater in the mild NPDR group compared to the NoDR group, perhaps due to the venodilation that occurs with development of DR. However, it is uncertain why the VD of larger vessels decreased again in the moderate NPDR group. A correlation between the Maximum entropy–based VD of larger vessels and automated AngioVue software-derived density may help in further characterization of the utility of this method. However, this was not possible in our study as our image acquisition was made using the automated tool in the TOPCON imaging system.

In case of DCP, there was a significant difference in VD noted with both Huang and Otsu algorithms between NoDR and mild NPDR groups and between NoDR and moderate NPDR groups, but not between mild NPDR and moderate NPDR groups. This suggests that changes in DCP-VD occur with development of even mild NPDR and are more consistently seen using various algorithms. Previous reports also suggest that the DCP gets affected earlier compared to SCP in DR,[22,23] and we believe that it was, therefore, found to be affected with both the thresholding methods in our study. The difference between mild and moderate NPDR may not be marked to achieve statistical significance in our study. This observation also goes hand in hand with the duration of diabetes in each group, with significantly greater duration observed in mild/moderate groups compared to NoDR group but no difference found between mild and moderate groups.

This study carries certain useful practical implications. First, different VD results are obtained with different thresholding algorithms, so one needs to check the algorithm before comparing the results of various studies. Second, the automated results may differ from the manual counts and should ideally not be compared in absolute values. Third, Huang segmentation method provided VD results that had moderately strong correlation with the automated results.

Fourth, Maximum entropy algorithm highlights the larger retinal vessels in SCP and may help in determining the vascular density of smaller vessels across which the actual perfusion occurs (VD of entire image − VD of larger vessels).

The study carries a few important limitations. First, the study population was not very large, and observations may have occurred due to chance. Following the strict inclusion and exclusion criteria, we could not get records of a very large number of patients. Severe NPDR patients were not included as they invariably had macular edema, which could have confounded the assessment. Second, proliferative DR cases were not included, and it would be interesting to know if the Huang method has good correlation and smaller limits of agreement in this category of cases. Third, we assessed only 3 × 3 mm area centered on the fovea, which may have been too small to detect meaningful difference consistently between the groups. Scans with a larger field may provide better information in this regard. However, the image resolution is generally inversely proportional to the scan size. Lastly, healthy (nondiabetic) controls could additionally have been used to compare the VD between various algorithms.

Conclusion

To conclude, this study highlights that the DCP-VD decreases with development of NPDR, as noted consistently with different thresholding algorithms. For SCP-VD analysis, more accurate algorithms need to be developed that can subtract the large vessels and depict the smaller VD accurately. The study puts forth an important question, that is, which is the best algorithm for quantitative vessel analysis using OCT-A? Probably, studies with histopathologic correlation can only provide an answer.

Conflicts of interest

There are no conflicts of interest.

References

1. Kashani AH, Chen C-L, Gahm JK, Zheng F, Richter GM, Rosenfeld PJ, *et al*. Optical coherence tomography angiography: A comprehensive review of current methods and clinical applications. Prog Retin Eye Res 2017;60:66–100.

2. Arfeen SA, Bahgat N, Adel N, Eissa M, Khafagy MM. Assessment of superficial and deep retinal vessel density in systemic lupus erythematosus patients using optical coherence tomography angiography. Graefes Arch Clin Exp Ophthalmol Albrecht Von Graefes Arch Klin Exp Ophthalmol 2020;258:1261-8.

3. O'Bryhim BE, Apte RS, Kung N, Coble D, Van Stavern GP. Association of preclinical alzheimer disease with optical coherence tomographic angiography findings. JAMA Ophthalmol 2018;136:1242–8.

4. Matsunaga DR, Yi JJ, De Koo LO, Ameri H, Puliafito CA, Kashani AH. Optical coherence tomography angiography of diabetic retinopathy in human subjects. Ophthalmic Surg Lasers Imaging Retina 2015;46:796–805.

5. de Carlo TE, Bonini Filho MA, Baumal CR, Reichel E, Rogers A, Witkin AJ, *et al*. Evaluation of preretinal neovascularization in proliferative diabetic retinopathy using optical coherence tomography angiography. Ophthalmic Surg Lasers Imaging Retina 2016;47:115–9.

6. Munk MR, Giannakaki-Zimmermann H, Berger L, Huf W, Ebneter A, Wolf S, *et al*. OCT-angiography: A qualitative and quantitative comparison of 4°CT-A devices. PloS One 2017;12:e0177059.

7. Toto L, Borrelli E, Mastropasqua R, Di Antonio L, Doronzo E, Carpineto P, *et al*. Association between outer retinal alterations and microvascular changes in intermediate stage age-related macular degeneration: An optical coherence tomography angiography study. Br J Ophthalmol 2017;101:774–9.

8. Lei J, Durbin MK, Shi Y, Uji A, Balasubramanian S, Baghdasaryan E, *et al*. Repeatability and reproducibility of superficial macular retinal vessel density measurements using optical coherence tomography angiography en face images. JAMA Ophthalmol 2017;135:1092–8.

9. Al-Sheikh M, Tepelus TC, Nazikyan T, Sadda SR. Repeatability of automated vessel density measurements using optical coherence tomography angiography. Br J Ophthalmol 2017;101:449–52.

10. Nesper PL, Roberts PK, Onishi AC, Chai H, Liu L, Jampol LM, *et al*. Quantifying microvascular abnormalities with increasing severity of diabetic retinopathy using optical coherence tomography angiography. Invest Ophthalmol Vis Sci 2017;58:BIO307–15.

11. Cicinelli MV, Rabiolo A, Marchese A, de Vitis L, Carnevali A, Querques L, *et al*. Choroid morphometric analysis in non-neovascular age-related macular degeneration by means of optical coherence tomography angiography. Br J Ophthalmol 2017;101:1193–200.

12. Chidambara L, Gadde SGK, Yadav NK, Jayadev C, Bhanushali D, Appaji AM, *et al*. Characteristics and quantification of vascular changes in macular telangiectasia type 2 on optical coherence tomography angiography. Br J Ophthalmol 2016;100:1482–8.

13. Iafe NA, Phasukkijwatana N, Chen X, Sarraf D. Retinal capillary density and foveal avascular zone area are age-dependent: Quantitative analysis using optical coherence tomography angiography. Invest Ophthalmol Vis Sci 2016;57:5780–7.

14. Wang JC, Laíns I, Providência J, Armstrong GW, Santos AR, Gil P, *et al*. Diabetic choroidopathy: Choroidal vascular density and volume in diabetic retinopathy with swept-source optical coherence tomography. Am J Ophthalmol 2017;184:75–83.

15. Ghasemi Falavarjani K, Tian JJ, Akil H, Garcia GA, Sadda SR, Sadun AA. Swept-source optical coherence tomography angiography of the optic disk in optic neuropathy. Retina Phila Pa 2016;36(Suppl 1):S168–77.

16. Akil H, Huang AS, Francis BA, Sadda SR, Chopra V. Retinal vessel density from optical coherence tomography angiography to differentiate early glaucoma, pre-perimetric glaucoma and normal eyes. PLoS One 2017;12:e0170476.

17. Rabiolo A, Gelormini F, Sacconi R, Cicinelli MV, Triolo G, Bettin P, *et al*. Comparison of methods to quantify macular and peripapillary vessel density in optical coherence tomography angiography. PLoS One 2018;13:e0205773.

18. Chu Z, Gregori G, Rosenfeld PJ, Wang RK. Quantification of choriocapillaris with optical coherence tomography angiography:

19. Mehta N, Liu K, Alibhai AY, Gendelman I, Braun PX, Ishibazawa A, *et al*. Impact of binarization thresholding and brightness/contrast adjustment methodology on optical coherence tomography angiography image quantification. Am J Ophthalmol 2019;205:54–65.

20. Schindelin J, Rueden CT, Hiner MC, Eliceiri KW. The ImageJ ecosystem: An open platform for biomedical image analysis. Mol Reprod Dev 2015;82:518–29.

21. Giedt RJ, Koch PD, Weissleder R. Single cell analysis of drug distribution by intravital imaging. PLoS One 2013;8:e60988.

22. Mastropasqua R, Toto L, Mastropasqua A, Aloia R, De Nicola C, Mattei PA, *et al*. Foveal avascular zone area and parafoveal vessel density measurements in different stages of diabetic retinopathy by optical coherence tomography angiography. Int J Ophthalmol 2017;10:1545–51.

23. Agemy SA, Scripsema NK, Shah CM, Chui T, Garcia PM, Lee JG, *et al*. Retinal vascular perfusion density mapping using optical coherence tomography angiography in normals and diabetic retinopathy patients. Retina Phila Pa 2015;35:2353–63.

24. Kim AY, Chu Z, Shahidzadeh A, Wang RK, Puliafito CA, Kashani AH. Quantifying microvascular density and morphology in diabetic retinopathy using spectral-domain optical coherence tomography angiography. Invest Ophthalmol Vis Sci 2016;57:OCT362-70.

25. Al-Sheikh M, Ghasemi Falavarjani K, Akil H, Sadda SR. Impact of image quality on OCT angiography based quantitative measurements. Int J Retina Vitreous 2017;3:13.

26. Dimitrova G, Chihara E, Takahashi H, Amano H, Okazaki K. Quantitative retinal optical coherence tomography angiography in patients with diabetes without diabetic retinopathy. Invest Ophthalmol Vis Sci 2017;58:190–6.

27. Otsu N. A threshold selection method from gray-level histograms. IEEE Trans Syst Man Cybern 1979;9:62–6.

28. Huang L-K, Wang M-JJ. Image thresholding by minimizing the measures of fuzziness. Pattern Recognit 1995;28:41–51.

29. Nguyen TT, Wang JJ, Sharrett AR, Islam FMA, Klein R, Klein BEK, *et al*. Relationship of retinal vascular caliber with diabetes and retinopathy: The Multi-Ethnic Study of Atherosclerosis (MESA). Diabetes Care 2008;31:544–9.

30. Shilova OG, Filippova S, Shilov M, Zapuskalov I. Evaluation of vascular system of the retina using ImageJ software. Invest Ophthalmol Vis Sci 2011;52:1281.

31. Holló G. Influence of removing the large retinal vessels–related effect on peripapillary vessel density progression analysis in glaucoma. J Glaucoma 2018;27:e137.

32. Maximum Entropy Threshold. ImageJ. Available from: https://imagej.net/Maximum_Entropy_Threshold. [Last accessed on 2018 Dec 22].

33. Sahoo PK, Soltani S, Wong AKC. A survey of thresholding techniques. Comput Vis Graph Image Process 1988;41:233–60.